Journal of ELECTRICAL ENGINEERING, VOL. 57, NO. 7/s, 2006, 9–13

SEMI–IMPLICIT FINITE VOLUME SCHEMES FOR SOLVING TENSOR DIFFUSION IN IMAGE PROCESSING

Oľga Drblíková *

This report deals with diamond cell finite volume scheme for tensor diffusion in image processing. First, we provide some basic information about this type of diffusion including a construction of its diffusion tensor. Then we derive a semi-implicit finite volume scheme for this non-linear model. Further, the proof of existence and uniqueness of a solution at each discrete time step is given. The main idea of this proof is a bounding of a gradient in tangential direction by a gradient in normal direction. Finally, we discuss computational results illustrated in figures.

K e y w o r d s: finite volume method, image processing, nonlinear parabolic equation, tensor diffusion

2000 *Mathematics Subject Classification*: 35K60, 94A08, 74S10

1 INTRODUCTION

Effort to gain processed image more quickly and not in a way computationally expensive leads to inventions of new diffusion models and also to their improvements. One of them was introduced by Weickert (see, e.g. [7]) in the following form

$$\frac{\partial u}{\partial t} - \nabla \cdot (D \nabla u) = 0\,, \qquad \text{in } Q_T \equiv I \times \Omega\,, \quad (1)$$

$$u(x,0) = u_0(x)\,, \qquad \text{in } \Omega\,, \quad (2)$$

$$\langle D \nabla u, n \rangle = 0\,, \qquad \text{on } I \times \partial\Omega\,, \quad (3)$$

where D is a matrix depending on the eigenvalues and on the eigenvectors of the so-called (regularized) structure tensor $J = \nabla u (\nabla u)^T$ (for details see next section). This modification is useful in any situation, where is desirable strong smoothing in one direction and low smoothing in the perpendicular direction. Owing to this property, tensor anisotropic diffusion has applied mainly for images with interrupted coherence of structures.

We derive our numerical scheme for this diffusion model by finite volume method. We choose this modern discretization technique since it is well suited for a numerical solution of conservation laws. It has been successfully applied in image processing, e.g. for solving the Perona-Malik equation [6] or curvature driven level set equation [5].

2 DERIVATION OF THE DIFFUSION TENSOR

2.1 Analysing coherent structures

In order to enhance a coherence of structures, we need a reliable tool for analysing coherent structures.

A very simple structure descriptor is given e.g. by the properties of $\nabla u_{\tilde{t}}$, where

$$u_{\tilde{t}}(x,t) = (G_{\tilde{t}} * u(\cdot,t))(x) \quad (\tilde{t} > 0)\,. \quad (4)$$

We can use e.g. absolute value of $\nabla u_{\tilde{t}}$ for detecting edges in some images (see [1]) but for images with line structures this descriptor is unuseful. One way of gaining the structure descriptor invariant under sign changes is to replace $\nabla u_{\tilde{t}}$ by its tensor product. Then we again average it by applying other convolution with Gaussian G_ρ

$$J_\rho(\nabla u_{\tilde{t}}) = G_\rho * (\nabla u_{\tilde{t}} \nabla u_{\tilde{t}}^\top) \qquad (\rho \geq 0)\,. \quad (5)$$

In computer vision community the matrix

$$J_\rho = \begin{pmatrix} a & b \\ b & c \end{pmatrix}$$

is well-known as structure tensor. This matrix J_ρ is symmetric and positive semidefinite and its eigenvalues are

$$\mu_{1,2} = \frac{1}{2}\left((a + c \pm \sqrt{(a-c)^2 + 4b^2})\right)\,, \quad \mu_1 \geq \mu_2\,. \quad (6)$$

The eigenvalues describe the average contrast in the eigendirections v and w.

The corresponding orthonormal set of eigenvectors (v, w) to eigenvalues (μ_1, μ_2) is given by

$$\begin{gathered} v = (v_1, v_2)\,, \qquad w = (w_1, w_2)\,, \\ v_1 = 2b\,, \quad v_2 = c - a + \sqrt{(a-c)^2 + 4b^2}\,, \\ w \perp v\,, \quad w_1 = -v_2\,, \quad w_2 = v_1\,. \end{gathered} \quad (7)$$

The orientation of the eigenvector w, which corresponds to the smaller eigenvalue μ_2, is called coherence orientation. This orientation has the lowest fluctuations.

2.2 Coherence-enhancing anisotropic diffusion

Since we have a tool for analysing coherence, we draw our goals to enhance image coherence. One of possibilities of doing it, can be done by embedding the structure tensor analysis into a non-linear diffusion filter.

* Slovak University of Technology, Faculty of Civil Engineering, Department of Mathematics and Descriptive Geometry, Radlinského 11, 813 68 Bratislava. E-mail: drblikov@math.sk

ISSN 1335-3632

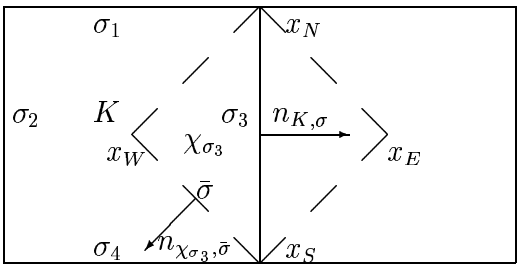

Fig. 1. A detail of a mesh — a finite volume K, its boundaries σ_i, $i = 1,2,3,4$ and covolume χ_{σ_3} corresponding to σ_3.

For enhancing coherence, the diffusion tensor D must steer a filtering process such that diffusion is strong mainly along the coherence direction w and it increases with the coherence $(\mu_1 - \mu_2)^2$. To obtain it, we require that D must possess the same eigenvectors v and w as the structure tensor $J_\rho(\nabla u_{\tilde{t}})$ and we choose the eigenvalues of D as

$$\kappa_1 = \alpha, \quad \alpha \in (0,1),\ \alpha \ll 1,$$

$$\kappa_2 = \begin{cases} \alpha, & \text{if } \mu_1 = \mu_2, \\ \alpha + (1-\alpha)\exp\left(\frac{-C}{(\mu_1-\mu_2)^2}\right), & C > 0 \text{ otherwise.} \end{cases}$$

The diffusion tensor D has a form

$$D = ABA^{-1} = \begin{pmatrix} \lambda & \beta \\ \beta & \nu \end{pmatrix}, \tag{8}$$

where $A = \begin{pmatrix} v_1 & -v_2 \\ v_2 & v_1 \end{pmatrix}$ and $B = \begin{pmatrix} \kappa_1 & 0 \\ 0 & \kappa_2 \end{pmatrix}$.

Due to the convolutions in (4) and (5), the elements of matrix D are C^1 functions.

3 FINITE VOLUME SCHEME FOR TENSOR ANISOTROPIC DIFFUSION IN IMAGE PROCESSING

The aim of this section is to prove existence of unique discrete solution for the model (1)–(3) which satisfies to semi-implicit finite volume scheme obtained with the help of co-volume mesh. Let us consider a rectangular image domain $\Omega = (0, n_1) \times (0, n_2)$ and let an image $u(x)$ be represented by a bounded mapping $u\colon \Omega \to R$. Our image is represented by $n_1 \times n_2$ pixels (finite volumes) such that it looks as mesh with n_1 rows and n_2 columns. We consider it in a scaling(time) interval $I = [0,T]$. Let $0 = t_0 \le t_1 \le \cdots \le t_{N_{\max}} = T$ denote the time discretization with $t_n = t_{n-1} + k$, where k is the time (scale) step. For $n = 0, \ldots, N_{\max}$ we will look for u^n an approximation of solution at time t_n.

We integrate equation (1) over finite volume K, provide a semi-implicit in time discretization and use a divergence theorem to get

$$\frac{u_K^n - u_K^{n-1}}{k} m(K) - \sum_{\sigma \in \mathcal{E}_K} \int_\sigma D^{n-1} \nabla u^n \cdot \mathbf{n}_{K,\sigma} \mathrm{d}s = 0, \tag{9}$$

where u_K^n, $K \in \mathcal{T}_h$ represents the mean value of u^n on K, $m(K)$ is the measure of the finite volume K with boundary ∂K, $\sigma_{KL} = K \cap L = K|L$ is an edge of the finite volume K, where $L \in \mathcal{T}_h$ is an adjacent finite volume to K such that $m(K \cap L) \neq 0$. Let us note that due to simpler notation, we will write in the sequel σ instead of σ_{KL}. $\mathcal{E}_K$ is a subset of $\mathcal{E}$ such that $\partial K = \bigcup_{\sigma \in \mathcal{E}_K} \sigma$, $\mathcal{E} = \bigcup_{K \in \mathcal{T}_h} \mathcal{E}_K$, where $\mathcal{T}_h$ is admissible finite volume mesh (see [4]). Υ is the set of pairs of adjacent finite volumes, defined by $\Upsilon = \{(K,L) \in \mathcal{T}_h^2,\ K \neq L,\ m(K|L) \neq 0\}$. We will denote D_σ^{n-1} as mean value of $D^{n-1} \equiv D(u^{n-1})$ on σ, that is $D_\sigma^{n-1} = \frac{1}{m(\sigma)} \int_\sigma D^{n-1} \mathrm{d}x$, where $m(\sigma)$ is the measure of edge σ, and $\mathbf{n}_{K,\sigma}$ is the normal unit vector to σ outward to K. Let us define the discrete solution by

$$u_{h,k}(x,t) = \sum_{n=0}^{N_{\max}} \sum_{K \in \mathcal{T}_h} u_K^n \chi\{x \in K\} \chi\{t_{n-1} < t \le t_n\}, \tag{10}$$

where the function $\chi(A)$ is defined as

$$\chi_{\{A\}} = \begin{cases} 1, & \text{if } A \text{ is true,} \\ 0, & \text{elsewhere.} \end{cases}$$

The extension of the function (10) outside Ω is given by its periodic mirror reflection to $\Omega_{\tilde{t}}$, where $\tilde{t}$ is the width of the smoothing kernel and

$$\Omega_{\tilde{t}} = \Omega \cup B_{\tilde{t}}(x), \quad x \in \partial\Omega. \tag{11}$$

$B_{\tilde{t}}(x)$ is a ball centered at x with radius $\tilde{t}$. We extend this periodic mirror reflection by 0 outside $\Omega_{\tilde{t}}$ and denote it by $\tilde{u}_{h,k}$. In order to get an approximation of equation (9) we write it in the form

$$\frac{u_K^n - u_K^{n-1}}{k} - \frac{1}{m(K)} \sum_{\sigma \in \mathcal{E}_K} \phi_\sigma^n(u_{h,k}^n) m(\sigma) = 0, \tag{12}$$

where $\phi_\sigma^n(u_{h,k}^n)$ denotes an approximation of the exact flux $\frac{1}{m(\sigma)} \int_\sigma D_\sigma^{n-1} \nabla u^n \cdot \mathbf{n}_{K,\sigma} \mathrm{d}s$ and $u_{h,k}^n(x) = \sum_{K \in \mathcal{T}_h} u_K^n \chi\{x \in K\}$.

One possibility of constructing $\phi_\sigma^n(u_{h,k}^n)$ is obtained with the help of co-volume mesh. The specific name (diamond-cell) of this method (see [2]) is due to the choice of co-volume as a diamond-shaped polygon. The co-volume χ_σ associated to σ is constructed around each edge by joining all four co-volume vertices (i.e. endpoints of this edge and midpoints of finite volumes which are common to this edge) (see Fig. 1). We denote the endpoints of an edge $\bar{\sigma} \subset \partial\chi_\sigma$ by $N_1(\bar{\sigma})$ and $N_2(\bar{\sigma})$ and $\mathbf{n}_{\chi_\sigma,\bar{\sigma}}$ is the normal unit vector to $\bar{\sigma}$ outward to χ_σ. In order to have an approximation of the diffusion flux, we first derive, using divergence theorem, an approximation of the averaged gradient on σ

$$\frac{1}{m(\chi_\sigma)} \int_{\chi_\sigma} \nabla u^n \mathrm{d}x = \frac{1}{m(\chi_\sigma)} \int_{\partial\chi_\sigma} u^n \mathbf{n}_{\chi_\sigma,\bar{\sigma}} \mathrm{d}s$$

and then we denote it by

$$p_\sigma^n = \frac{1}{m(\chi_\sigma)} \sum_{\bar\sigma \in \partial\chi_\sigma} \frac{1}{2}\big(u^n_{N_1(\bar\sigma)} + u^n_{N_2(\bar\sigma)}\big) m(\bar\sigma)\mathbf{n}_{\chi_\sigma,\bar\sigma}\,.$$

The value at the centres x_E and x_W are u_E and u_W while the values at the vertices x_N and x_S are computed as the arithmetic mean of values on finite volumes which are common to this vertex (for general non-uniform meshes see [2]).

Since our mesh is uniform squared, for simplification, we can use the following relations: $m(\chi_\sigma) = \frac{h^2}{2}$, $m(\bar\sigma) = \frac{\sqrt{2}}{2}h$ and after a short calculation we are ready to write

$$p_\sigma^n = \frac{u_E^n - u_W^n}{h}\mathbf{n}_{K,\sigma} + \frac{u_N^n - u_S^n}{h}\mathbf{t}_{K,\sigma}\,, \qquad (13)$$

where $\mathbf{t}_{K,\sigma}$ is a unit vector parallel to σ such that $(x_N - x_S)\cdot\mathbf{t}_{K,\sigma} > 0$. Although such u_N^n, u_W^n, u_E^n and u_S^n correspond to particular edge σ, we should denote them by $u^n_{N_\sigma}$, $u^n_{W_\sigma}$, $u^n_{E_\sigma}$ and $u^n_{S_\sigma}$, but we use those simpler notations. Replacing the exact gradient ∇u^n by the numerical gradient p_σ^n we get the numerical flux in the form

$$\phi_\sigma^n(u_{h,k}^n) = \frac{1}{m(\sigma)}\int_\sigma D^{n-1}p_\sigma^n\cdot\mathbf{n}_{K,\sigma}\,\mathrm{d}s = D_\sigma p_\sigma^n\cdot\mathbf{n}_{K,\sigma}\,, \qquad (14)$$

where $D_\sigma = \frac{1}{m(\sigma)}\int_\sigma D^{n-1}\mathrm{d}s = \begin{pmatrix}\bar\lambda_\sigma & \bar\beta_\sigma\\ \bar\beta_\sigma & \bar\nu_\sigma\end{pmatrix}$ in the basis $(\mathbf{n}_{K,\sigma},\mathbf{t}_{K,\sigma})$. It means, if $D = \begin{pmatrix}\lambda & \beta\\ \beta & \nu\end{pmatrix}$ then $D_{\sigma_2} = D_{\sigma_3} = \begin{pmatrix}\lambda_\sigma & \beta_\sigma\\ \beta_\sigma & \nu_\sigma\end{pmatrix}$, i.e. $\bar\lambda_\sigma = \lambda_\sigma$, $\bar\beta_\sigma = \beta_\sigma$, $\bar\nu_\sigma = \nu_\sigma$. On the other hand, $D_{\sigma_1} = D_{\sigma_4} = \begin{pmatrix}\nu_\sigma & -\beta_\sigma\\ -\beta_\sigma & \lambda_\sigma\end{pmatrix}$, i.e. $\bar\lambda_\sigma = \nu_\sigma$, $\bar\beta_\sigma = -\beta_\sigma$, $\bar\nu_\sigma = \lambda_\sigma$, where $\lambda_\sigma = \frac{1}{m(\sigma)}\int_\sigma \lambda^{n-1}\mathrm{d}s$ and β_σ and ν_σ correspondingly. Definition (14) can be also written in this form

$$\phi_\sigma^n(u_{h,k}^n) = \begin{pmatrix}\bar\lambda_\sigma & \bar\beta_\sigma\\ \bar\beta_\sigma & \bar\nu_\sigma\end{pmatrix}\begin{pmatrix}\frac{u_E^n - u_W^n}{h}\\ \frac{u_N^n - u_S^n}{h}\end{pmatrix}\cdot\begin{pmatrix}1\\0\end{pmatrix} = \bar\lambda_\sigma\frac{u_E^n - u_W^n}{h} + \bar\beta_\sigma\frac{u_N^n - u_S^n}{h}\,, \qquad (15)$$

since (13) in the basis $(\mathbf{n}_{K,\sigma},\mathbf{t}_{K,\sigma})$ can be for each edge written as

$$p_\sigma^n = \begin{pmatrix}\frac{u_E^n - u_W^n}{h}\\ \frac{u_N^n - u_S^n}{h}\end{pmatrix} \qquad (16)$$

and $\mathbf{n}_{K,\sigma}$ in the basis $(\mathbf{n}_{K,\sigma},\mathbf{t}_{K,\sigma})$ is equal to $(1\quad 0)^\top$ for all edges.

In order to prove of existence and uniqueness of u_K^n, $K\in\mathcal{T}_h$, we estimate the expressions $u_N^n - u_S^n$ by means of $u_E^n - u_W^n$ for all edges σ in the following form

$$\sum_{\sigma\in\mathcal{E}_{int}}\Big(\frac{\bar\beta_\sigma}{\bar\lambda_\sigma}\Big)^2\Big(\frac{u_N - u_S}{h}\Big)^2\bar\lambda_\sigma \le \gamma\sum_{\sigma\in\mathcal{E}}\Big(\frac{u_E - u_W}{h}\Big)^2\bar\lambda_\sigma\,, \qquad (17)$$

where

$$0\le\gamma<1\,,\quad \gamma = \max_{\sigma\in\mathcal{E}}\gamma_\sigma\,,\quad \gamma_\sigma = \frac{(\beta_\sigma)^2}{\lambda_\sigma\nu_\sigma}(1+O(h)) \qquad (18)$$

for h sufficiently small (for details see [3]).

Let us now introduce the space of piecewise constant functions associated to our mesh and discrete H^1 norm for this space. This discrete norm will be used to obtain some estimates on the approximate solution given by a finite volume scheme.

Definition 1. Let Ω be an open bounded polygonal subset of R^2. We define $\mathcal{P}_0(\mathcal{T}_h)$ as the set of functions from Ω to R which are constant over each finite volume of the mesh.

Definition 2. Let Ω be an open bounded polygonal subset of R^2. For $u\in\mathcal{P}_0(\mathcal{T}_h)$ we define

$$|u_{h,k}^n|_{1,\mathcal{T}_h} = \Big(\sum_{(K,L)\in\Upsilon}\frac{(u_L - u_K)^2}{d_{K,L}}m(\sigma)\Big)^{\frac{1}{2}}, \qquad (19)$$

where $d_{K,L}$ is the Euclidean distance between x_K and x_L.

Note that (19) can be rewritten for our uniform mesh into the following form

$$|u_{h,k}^n|_{1,\mathcal{T}_h} = \Big(2\sum_{\sigma\in\mathcal{E}}\Big(\frac{u_E - u_W}{h}\Big)^2 m(\chi_\sigma)\Big)^{\frac{1}{2}}. \qquad (20)$$

We can define discrete operator for (1)–(3) by

$$\mathcal{L}_h(u_{h,k}^n) = u_K^n m(K) - k\sum_{\sigma\in\mathcal{E}_K}\phi_\sigma^n(u_{h,k}^n)m(\sigma)\,, \qquad (21)$$

such that $u_{h,k}^n$ is the solution in $\mathcal{P}_0(\mathcal{T}_h)$ of

$$\mathcal{L}_h(u_{h,k}^n) = f_{h,k}(u_{h,k}^{n-1})\,, \qquad (22)$$

where $f_{h,k}(u_{h,k}^{n-1}) = u_K^{n-1}m(K)$ and u_K^{n-1} is a value of the piecewise constant function $u_{h,k}^{n-1}$ in K. This equality is a linear system of N equations with N unknowns, namely u_K^n, $K\in\mathcal{T}_h$, where $N = \mathrm{card}(K)$. Multiplying $\mathcal{L}_h(u_{h,k})$ by u_K^n, summing over K and splitting into a part A and B leads to

$$\sum_{K\in\mathcal{T}_h}\mathcal{L}_h(u_{h,k}^n)u_K^n = A + B\,, \qquad (23)$$

with

$$A = \sum_{K\in\mathcal{T}_h}(u_K^n)^2 m(K) = ||u_{h,k}^n||^2_{L^2(\Omega)}\,, \qquad (24)$$

$$B = k\sum_{K\in\mathcal{T}_h}u_K^n\sum_{\sigma\in\mathcal{E}_K} -\phi_\sigma^n(u_{h,k}^n)m(\sigma)\,. \qquad (25)$$

Then we bound $\sum_{K\in\mathcal{T}_h}\mathcal{L}_h(u_{h,k}^n)u_K^n$ as follows

$$\sum_{K\in\mathcal{T}_h}\mathcal{L}_h(u_{h,k}^n)u_K^n \ge \alpha\big(|u_{h,k}^n|^2_{1,\mathcal{T}_h} + ||u_{h,k}^n||^2_{L^2(\Omega)}\big) \qquad (26)$$

with $\alpha = \min\big(\bar\lambda_{\min}(1-\gamma)\frac{k}{2}, 1\big)$, where $\bar\lambda_{\min} = \inf_{\sigma\in\mathcal{E}}\bar\lambda_\sigma \ge C > 0$ (for details of derivation of this inequality see [3]).

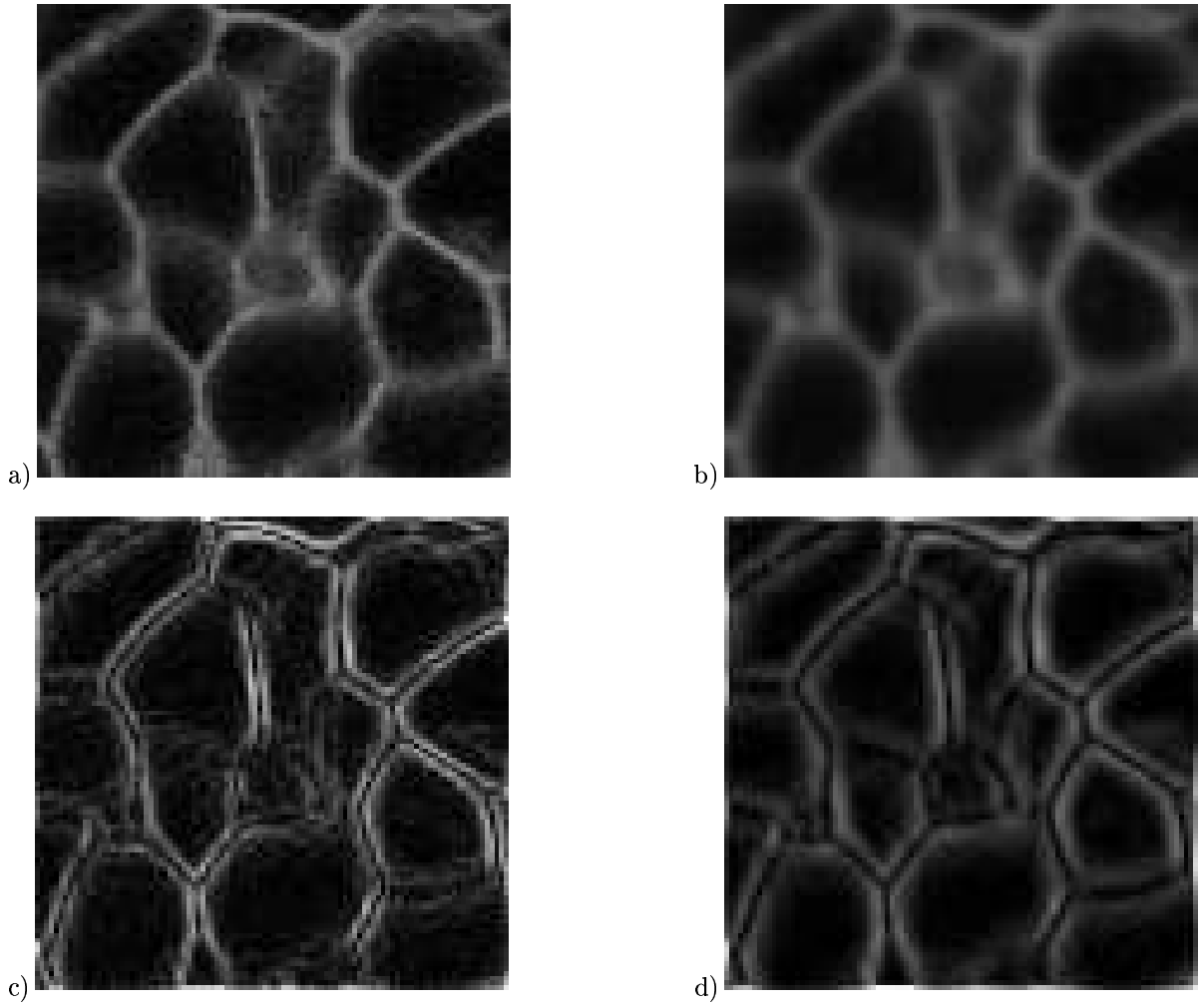

Fig. 2. Cell membranes. The image size is 100×100 pixels. a) an original image, b) an image after 1000 steps with time step $k = 0.0001$, c) an edge detection for an original image, d) an edge detection for an image after 1000 steps.

Theorem 3. *For h sufficiently small, there exists a unique solution $u_{h,k}$ given by scheme (12) with (15).*

P r o o f . Assume that $u_{h,k}$ satisfies the linear system (22) and let $f = 0$. Using (26) and (22) we get

$$\alpha\big(|u^n_{h,k}|^2_{1,\mathcal{T}_h} + ||u^n_{h,k}||^2_{L^2(\Omega)}\big) \leq \sum_{K\in\mathcal{T}_h} \mathcal{L}_h(u^n_{h,k})u^n_K = \sum_{K\in\mathcal{T}_h} f u^n_K = 0\,. \quad (27)$$

Due to relation (27), we know that $u^n_K = 0$, $\forall K \in \mathcal{T}_h$. It means that kernel of the linear transformation represented by the matrix of the system (22) contains only $\bar{0}$ vector, which implies that the matrix is regular. And thus it implies that there exists a unique solution for any right hand side.

4 NUMERICAL EXPERIMENTS

In this section we present some results of image filtering. We illustrate behaviour of the tensor diffusion, using our scheme (12) with the numerical flux given by (15), in two examples.

We have chosen the parameters of our scheme in the following way $C = 1$ and $\alpha = 0.001$. In our implementation $k = 0.0001$ and $h = 1/n1$, where $n1 \times n2$ is the number of pixels. The arising sparse linear systems are solved by Gauss-Seidel iterative method. For numerical implementation we use programming language C.

The images used for our numerical experiments were obtained by multiphoton laser scanning microscopy. They are chosen from series of images which show a processes of animal embryogenesis. The experiments documented in Figs. 2 and 3 were performed on the greyscale images of size 100×100 pixels (Fig. 2) and 240×240 pixels (Fig. 3).

As a demonstration we present Figs. 2, 3. In Fig. 2, cell membranes of the head of a 24 hours embryo are depicted while Fig. 3 illustrates cells with nuclei of the head of a 3 hours embryo. Both Figs. 2 and 3 consist of four sub-figures. For each of these figures, at the top (left) we show cells visualized using the original noisy data, at the top (right) the result of smoothing after 1000 (Fig. 2) and 300 discrete time steps (Fig. 3), at the bottom (left) an edge detection corresponds to the original image and at the bottom (right) an edge detection corresponds to the filtered image.

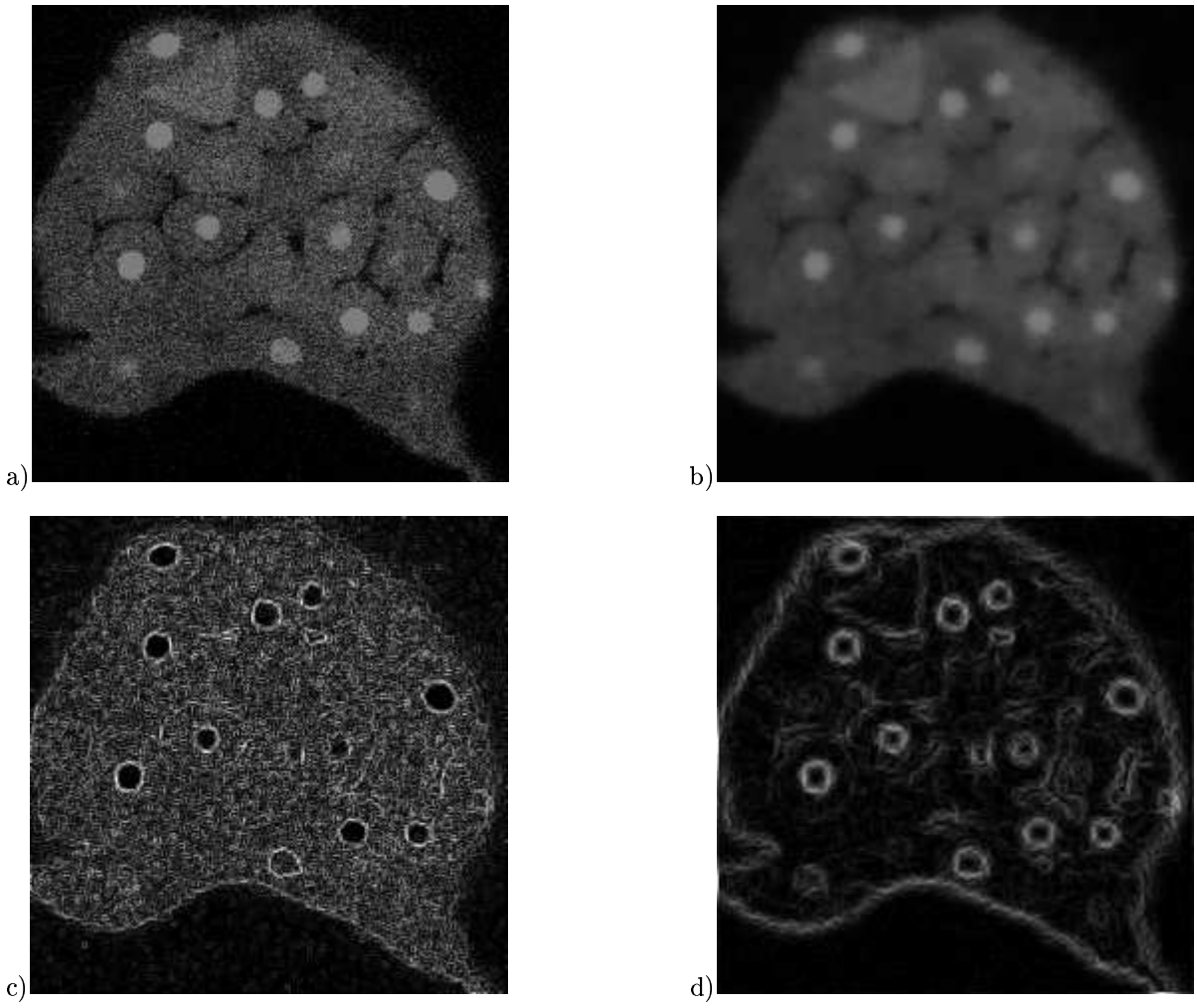

Fig. 3. Cells with nuclei. The image size is 240×240 pixels. a) an original image, b) an image after 300 steps with time step $k = 0.0001$, c) an edge detection for an original image, d) an edge detection for an image after 300 steps.

In these figures an effect of smoothing and emphasizing line structures can be observed. One can compare edge detections of the original (Figs. 2, 3 c) and filtered images (Figs. 2, 3 d). Even if filtered images (Figs. 2, 3 b) are more blurred compared with original images (Figs. 2, 3 a), we can see that line structures (boundaries of membranes and nuclei) (Figs. 2, 3 d) are clearly detected compared with the original images (Figs. 2, 3 c).

It shows that application of our numerical scheme gives suitably preprocessed images, e.g. for subsequent segmentation.

Acknowledgement

This work was supported by the grants VEGA 1/0313/03, APVT-20-040902 and European projects Embryomics and BioEmergences. We thank to Dr. Nadine Peyrieras from CNRS Paris for the testing images.

References

[1] CATTÉ, F.—LIONS, P. L.—MOREL, J. M.—COLL, T.: Image Selective Smoothing and Edge Detection by Nonlinear Diffusion, SIAM J. Numer. Anal. **129** (1992), 182–193.

[2] COUDIERE, Y.—VILA, J. P.—VILLEDIEU, P.: Convergence Rate of a Finite Volume Scheme for a Two-Dimensional Convection-Diffusion Problem, M2AN, Math. Model Numer. Anal. **33** (1999), 493–516.

[3] DRBLÍKOVÁ, O.: Finite Volume Schemes for Tensor Anisotropic Diffusion in Image Processing, Proceedings of MAGIA 2005, November 28–30, 2005, Kočovce, pp. 7–18.

[4] EYMARD, R.—GALLOUËT, T.—HERBIN, R.: Finite Volume Methods, in: Handbook for Numerical Analysis, Vol. 7 (Ph. Ciarlet, J.L. Lions, eds.), Elsevier, 2000.

[5] HANDLOVIČOVÁ, A.—MIKULA, K.—SGALLARI, F.: Semi-Implicit Complementary Volume Scheme for Solving Level Set Like Equations in Image Processing and Curve Evolution, Numer. Math. **93** No. 4 (2003), 675–695.

[6] MIKULA, K.—RAMAROSY, N.: Semi-Implicit Finite Volume Scheme for Solving Nonlinear Diffusion Equations in Image Processing, Numer. Math. **89** No. 3 (2001), 561–590.

[7] WEICKERT, J.: Coherence-Enhancing Diffusion Filtering, Internat. J. Comput. Vision **31** (1999), 111–127.

Received 17 May 2006

Oľga Drblíková (Mgr) graduated in Mathematics and Biology at the Faculty of Natural Sciences of the Comenius University, Bratislava. She works as a researcher at the Department of Mathematics and Descriptive Geometry at the Faculty of Civil Engineering of the Slovak University of Technology, Bratislava. She deals with computational methods based on non-linear diffusion in image processing. Her PhD supervisor is Assoc. Prof. Karol Mikula.